

# A unilateral magnet with an extended constant magnetic field gradient

Juan C. García-Naranjo<sup>a,b,c</sup>, Igor V. Mastikhin<sup>a</sup>, Bruce G. Colpitts<sup>b</sup>, Bruce J. Balcom<sup>a,\*</sup>

<sup>a</sup> MRI Centre, Department of Physics, P.O. Box 4400, University of New Brunswick, Fredericton, NB, Canada E3B 5A3

<sup>b</sup> Department of Electrical and Computer Engineering, P.O. Box 4400, University of New Brunswick, Fredericton, NB, Canada E3B 5A3

<sup>c</sup> Centre of Medical Biophysics, Universidad de Oriente, Patricio Lumumba S/N, Santiago de Cuba 90500, Cuba

## ARTICLE INFO

### Article history:

Received 1 July 2010

Revised 29 September 2010

Available online 7 October 2010

### Keywords:

Constant gradient

Unilateral magnetic resonance

Diffusion

Magnet design

Inhomogeneous field

Three magnet array

## ABSTRACT

Unilateral magnetic resonance (UMR) has become, in different research areas, a powerful tool to interrogate samples of arbitrary size. Numerous designs have been suggested in the literature to produce the desired magnetic field distributions, including designs which feature constant magnetic field gradients suitable for diffusion and profiling experiments. This work presents a new approach which features extended constant magnetic field gradients with a three magnet array. Constant gradients of more than 3 cm extent can be achieved in a very simple, compact and safe design. Diffusion measurements from different positions over the magnet are presented in addition to practical applications for reservoir core plug characterization. The idea of a solenoid as a probe for specific measurements in UMR is introduced. Simple profiling experiments are also presented.

© 2010 Elsevier Inc. All rights reserved.

## 1. Introduction

In recent years unilateral magnetic resonance (UMR) has become a powerful tool to explore samples of arbitrary size; permitting magnetic resonance experiments on more complex and challenging samples. A wide range of applications have been developed in different areas such as down-hole oil well logging [1], biomedicine [2], concrete materials analysis [3] and characterization of food products [4]. The first area of application is now ubiquitous in the oil industry.

Different magnet designs have been proposed to create an MR compatible static magnetic field. Three main classes can be easily differentiated taking into account the distribution of the static magnetic field. In the first class [5,6] the orientation of the magnets and RF coil are arranged in such a way that the grossly inhomogeneous  $B_0$  and  $B_1$  remain perpendicular in specific regions which, in conjunction with the RF excitation bandwidth, defines a sensitive spot for the measurement. A second class includes those magnets designed to produce a relatively homogeneous  $B_0$  field in a defined region of space [1,7–11]. This yields a large spot for RF excitation and reduces diffusive attenuation of gradients by molecular motion through underlying magnetic field.

The third class of unilateral magnets features a linear magnetic field distribution (constant gradient) in a region of interest which is suitable for profiling and diffusion measurements. Prado [12] presented a palm-size unilateral magnet design which includes

gradient coils. This design permits pulsed field gradients, making possible the application of pure phase encoding techniques. Blumich et al. [13] introduced a variation of the NMR-MOUSE employing a single bar magnet, with a constant gradient of around 2000 G/cm in its central part. This approach is very simple but the linear region of the magnetic field is limited to around 4 mm. Casanova and Blumich [14] and Perlo et al. [15] developed these ideas for 2D and 3D with an optimized design of the magnets, a set of switched magnetic field gradient and a new multi-echo sequence. Nevertheless, as in the Prado approach, these ideas require a power source to produce the desired magnetic field gradients.

Perlo et al. [16] more recently introduced a magnet with a permanent gradient of 2000 G/cm perpendicular to the magnet surface. As in the STRAFI technique [17], the major effort was focused on producing a very uniform spot in a plane parallel to the magnet surface. This homogeneous plane is achieved by doubling the number of magnets in the original MOUSE and improving their spatial distribution. Selection of the plane of measurement inside the sample is achieved by changing the position of the magnet relative to the sample. This approach can produce high resolution profiles, but requires a complex magnet design, with associated complexity of fabrication.

A different approach to unilateral magnetic resonance with a constant gradient was suggested by Marble et al. [18]. He advocated the use of a shaped pole piece to create a permanent gradient. Magnetic field gradients of 30–250 G/cm have been produced based on this idea.

In separate work, Marble et al. conceived a very simple approach [10] for producing a homogenous spot unilateral magnet.

\* Corresponding author. Fax: +1 506 453 4581.

E-mail address: [bjb@unb.ca](mailto:bjb@unb.ca) (B.J. Balcom).

This approach employs three simple magnet blocks, with the same field orientation, arranged along the same axis in a very safe (no repulsive forces) low energy configuration. In this way, the desired magnetic field distribution is achieved with a very compact design [19]. The natural field orientation,  $B_0$  parallel to the surface, permits more sensitive surface coils to be employed for RF excitation and detection. The relatively simple mathematical expressions required for calculating the field distribution make this approach very easy to simulate [10].

As outlined in this paper, vertical displacement of the central magnet block changes the design, from a uniform spot to an extended constant magnetic field gradient perpendicular to the magnet surface. Our desire is to create a new type of constant gradient unilateral magnet with a simple and robust design where the gradient is permanent. Practical measurements show that it is possible to generate constant gradients of more than 3 cm extent perpendicular to the magnet surface in a 1 cm diameter cylindrical volume.

In this paper we examine the properties of the constant gradient three magnet array through simulation and experiment. We introduce the idea of a simple solenoidal RF coil encompassing cylindrical samples to aid sensitivity and selective excitation of regions substantially removed from the magnet surface. Samples of particular interest include petroleum reservoir core plugs within which we measure molecular self diffusion of the saturating

fluid, exploiting the extended constant gradient in the sample space.

## 2. Theory

Our experimental goal is the creation of simple, low cost, magnet arrays where the RF magnetic field will be perpendicular to the magnet array surface, with the  $B_0$  field parallel. The magnetic field gradient is permanent, not switched, but may be readily adjusted by displacing the central magnet. This design permits the use of sensitive RF probes which may be surface coils or solenoids. In the latter case the long axis of the probe will be oriented in the  $x$  axis (see Fig. 1b). The solenoid naturally yields a more homogeneous  $B_1$  and will permit RF excitation over the full range of the constant magnetic field gradient permitting measurement at a wide range of depths into the sample.

### 2.1. Three magnet array

The distribution of the magnetic field over a three magnet array can be calculated by evaluating Eq. (1) in [10], for each single block of width  $w$  and height  $t$  and superposing the results according to their positions in the  $y$ - $z$  plane.

Fig. 1 presents a constant gradient magnet array built employing this approach. Magnet blocks with the same dimensions as

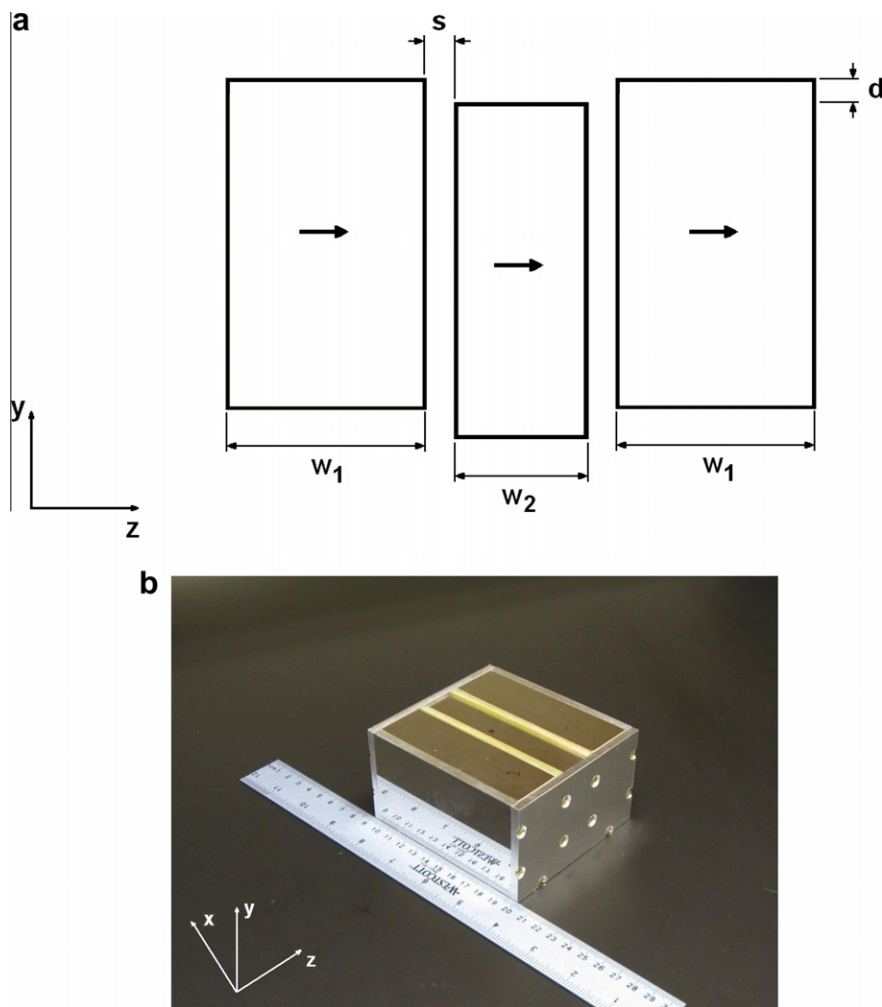


**Fig. 1.** Schematic (a) and photo (b) of the three magnet array. The static field  $B_0$  parallel to the array surface, is oriented in the  $z$  direction. The width of the external ( $w_1$ ) and central ( $w_2$ ) blocks is 3 cm and 2 cm respectively. The separation between blocks was set to 4.76 mm and the displacement of the central block ( $d$ ) is 2 mm for extended constant gradient.

those described in [10] were employed. Magnetic field compensation with a steel plate, as described in [10], was unnecessary.

It is straightforward, to calculate the first and second derivatives of the magnetic field produced by the three magnet array along the  $y$  axis. Nevertheless, it is more complex to calculate the zeros of the second derivative as a function of the physical dimensions of the magnet array. A simple numerical evaluation of this function is preferred.

## 2.2. Extended constant gradient

Evaluation of the first derivative (gradient) of the magnetic field on a vertical line ( $y$  axis) over the center of the array for a homogeneous spot design (solid line) is presented in Fig. 2. As can be observed, it is characterized by the presence of a maximum value, zero for homogeneous spot, followed by a minimum. The amplitude of the minimum, termed the natural gradient hereafter, principally depends on the separation between the external magnet blocks (measured from their central line) and therefore cannot be changed once the array is built. However, the amplitude of the maximum is more dependent on the position of the central block and can be easily changed by moving it up or down.

Fig. 2 presents the calculated magnetic field gradient for different positions of the central magnet block. As can be observed, different gradient values can be added to the sensitive spot (maximum of the curve) without a significant influence on the natural gradient. In fact, the central block can be displaced in such a way that the variable and natural gradients combine to produce an extended constant gradient with amplitude depending on the separation of the external blocks.

## 2.3. The probe

It is common practice in UMR to employ surface coils as the RF probe. As mentioned before, the orientation of the magnetic field produced by the three magnet array allows exploiting the high sensitivity of the circular loop probe. Nevertheless, in some applications it is desirable to explore deep layers inside the sample, which makes more challenging the employment of surface coils. Increasing its diameter to increase the penetration depth will make the coil more susceptible to external interference and other unde-

sirable effects but less sensitive to the desired signal through the principle of reciprocity.

In applications like rock core plug analysis, the shape of the sample suggests the employ of a solenoid oriented along the  $x$ -axis as the RF probe. It can be tailored to the sample, or a set of samples, in a very simple and well known way. For the three magnet array with extended constant gradient, the well controlled distribution of the magnetic field makes even simpler the employment of a solenoid which, in addition, will contribute with a very homogeneous  $B_1$ .

## 2.4. Diffusion measurements

Diffusion in the presence of a constant gradient has been studied by many laboratories employing the fringe field of superconducting magnets [20–23], well logging tools [24] and portable systems [25]. Obtaining constant gradients over an extended distance in a unilateral magnet is a very challenging design goal.

Different pulse sequences have also been employed for measuring diffusion [20,21,25] in static gradients. In this work the static gradient stimulated echo sequence with 16 phase cycle steps [21] is employed to characterize the gradient produced by the three magnet array. It is also exploited for measurements in realistic samples from petroleum reservoirs.

### 2.4.1. Static gradient stimulated echo sequence

The static gradient stimulated echo sequence (SGSTE) combined with CPMG (SGSTE-CPMG) as presented in Fig. 3 was introduced by Hurlimann and Venkataramanan [21] as a variation of the Laicher [26] approach for pulsed field gradient diffusion. Hurlimann added a 16 step phase cycling to select the contribution of the stimulated echo in order to obtain diffusion- $T_2$  distributions. The same sequence has been employed by Rata [25] for measuring diffusion with a reference acquisition at very short  $\tau_2$  as a normalization signal. In this case Eq. (1) was employed assuming no diffusive attenuation during the reference acquisition for a short  $\tau_2$ .

$$\ln\left(\frac{I}{I_0}\right) = -\gamma^2 G^2 D \tau_1^2 \left(\tau_2 + \frac{2}{3} \tau_1\right) \quad (1)$$

This assumption makes more complex the process of choosing the  $\tau_1$  values for the measurement. The SGSTE sequence, as described in [20], should be relaxation independent, which means that the  $\tau_1$  values during the acquisition process should be the same as those employed for the reference acquisition. Therefore, the longest  $\tau_1$  cannot be longer than  $\tau_2$  for the reference acquisition. At the same time the  $\tau_1$  values should be spaced sufficiently to differentiate the signal attenuation produced by the diffusion process from the noise.

A simple mathematical analysis of Eq. (2) [23] for the reference and the measurement acquisitions yields Eq. (3) for the normalized signal attenuation where  $\tau_{2r}$  is the  $\tau_2$  value employed for the reference acquisition.

$$M = \frac{M_0}{2} \exp \left\{ -\frac{\tau_2}{T_1} - \frac{2\tau_1}{T_2} - \gamma^2 D G^2 \tau_1^3 \left( \frac{2}{3} + \frac{\tau_2}{\tau_1} \right) \right\} \quad (2)$$

$$\ln\left(\frac{I}{I_r}\right) = -\frac{(\tau_2 - \tau_{2r})}{T_1} - \gamma^2 G^2 D \tau_1^2 (\tau_2 - \tau_{2r}) \quad (3)$$

For a chosen  $\tau_2$  the first addend is constant and the slope of the curve of attenuation versus  $\tau_1^2$  can be employed to calculate either the diffusion coefficient or the gradient. Even though this method requires an extra acquisition, the overall acquisition time can be reduced because of the increased SNR produced by averaging the CPMG echo train for both the reference and the measurement acquisitions.

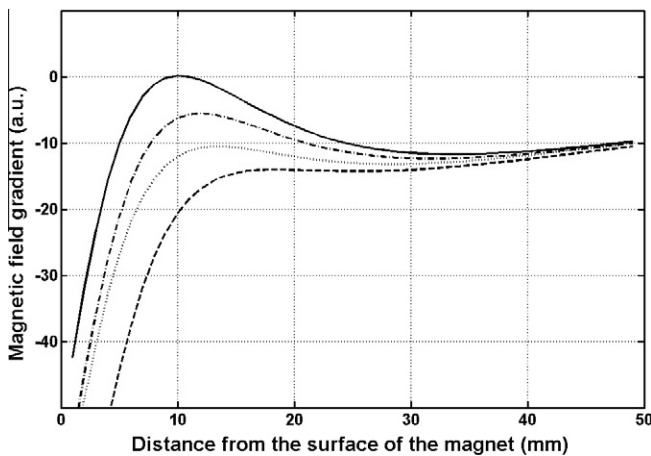


**Fig. 2.** Magnetic field gradient along a vertical line on the center of the array. A homogeneous spot design (solid) translates to an extent constant gradient design (dashed) by vertical displacement of the central block from 4.8 to 2 mm from the surface. Intermediate positions exhibit small regions, near 1 cm, of good linearity (variable gradient) at lower gradient values. The extended constant gradient is obtained by combining the variable (curve maximum) and natural (curve minimum) gradient of the array.

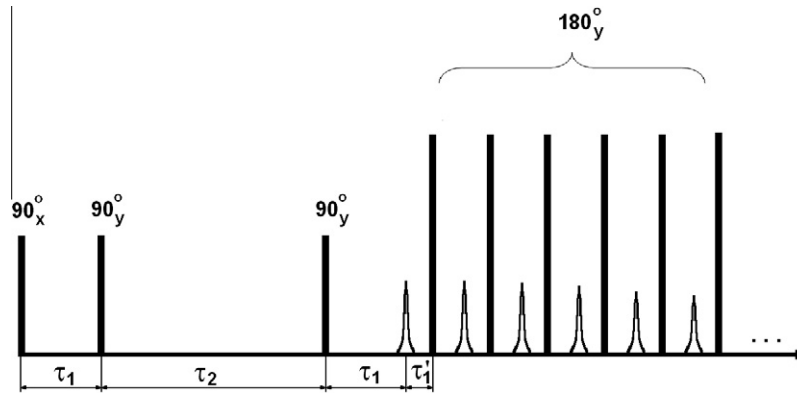


**Fig. 3.** SGSTE pulse sequence combined with CPMG. For each diffusion measurement eight  $\tau_1$  values were employed. A reference acquisition for  $\tau_2$  of 0.5 ms was also performed.

#### 2.4.2. Time-dependent diffusion coefficient

Diffusion measurements employing the SGSTE–CPMG sequence can be undertaken in order to obtain the volume to surface ratio ( $V/S$ ) in rock core plugs [25]. By varying the diffusion time ( $\tau_2$ ) water molecules are allowed to diffuse for a length  $L_D = \sqrt{D_0 \tau_2}$ . In porous media this distance is limited by the pore walls resulting in an apparently smaller diffusion coefficient. By plotting the apparent diffusion coefficient vs. diffusion length, the value of  $V/S$  can be obtained by assuming linear behavior for short diffusion lengths according to Eq. (4) [25].

$$D(L_D) \approx D_0 \left[ 1 - \frac{4}{9\sqrt{\pi}} \frac{L_D S}{V} \right] \quad (4)$$

### 3. Results and discussion

Fig. 4 presents the measured magnetic field over the prototype constant gradient magnet. The gradient strength is 218 G/cm over a constant region of 2.4 cm, with a maximum deviation of 1.5 G from linear behavior (Fig. 4a). The magnetic field measured

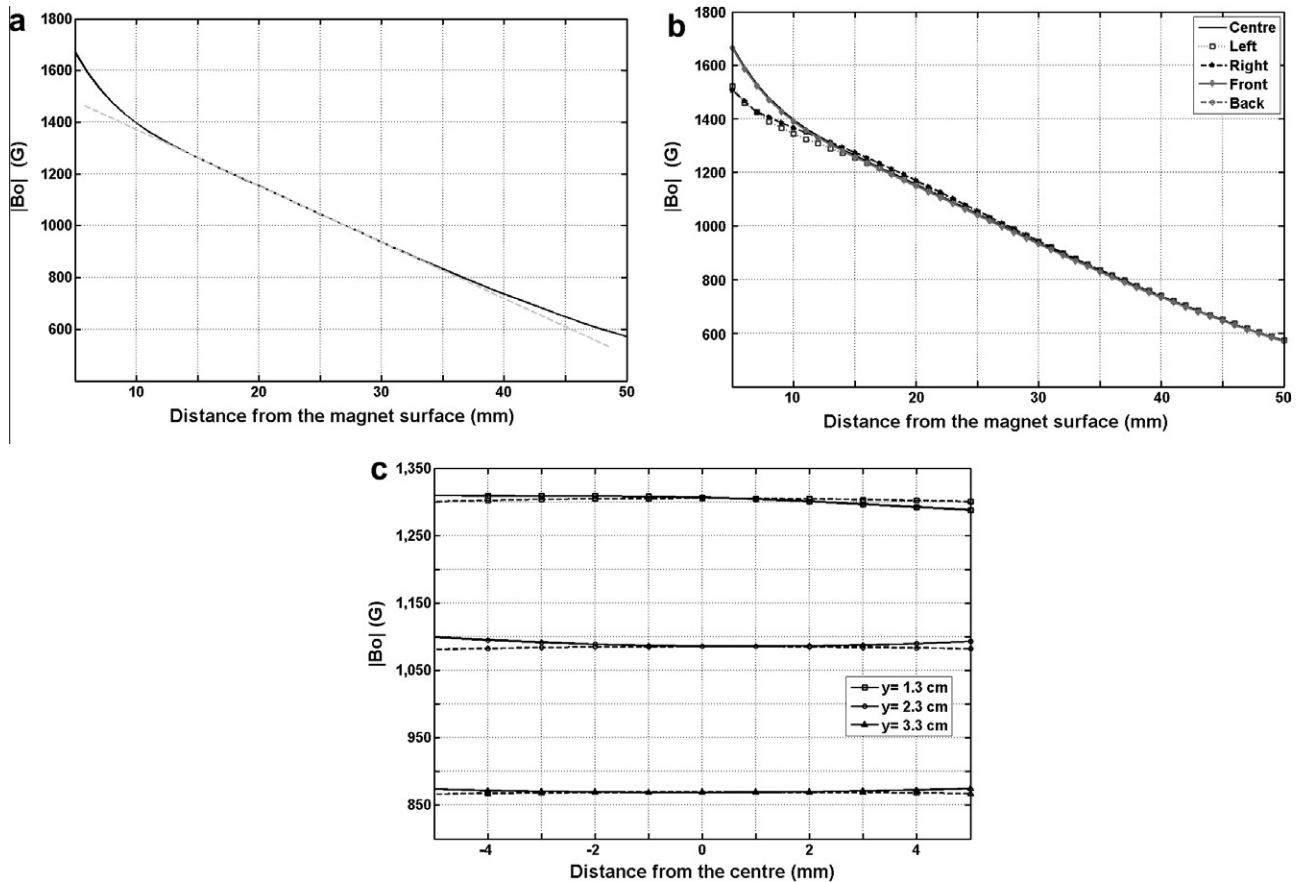


**Fig. 4.** Measured magnetic field over the magnet. The extended constant gradient of 218 G/cm at the center of the array is clearly observed in (a). The magnetic field on vertical lines spaced 5 mm from the center have been plotted in (b). The magnetic field along horizontal lines (c) at three heights over the magnet. Solid and dashed lines correspond to measurements along the  $z$  and  $x$  axes respectively.

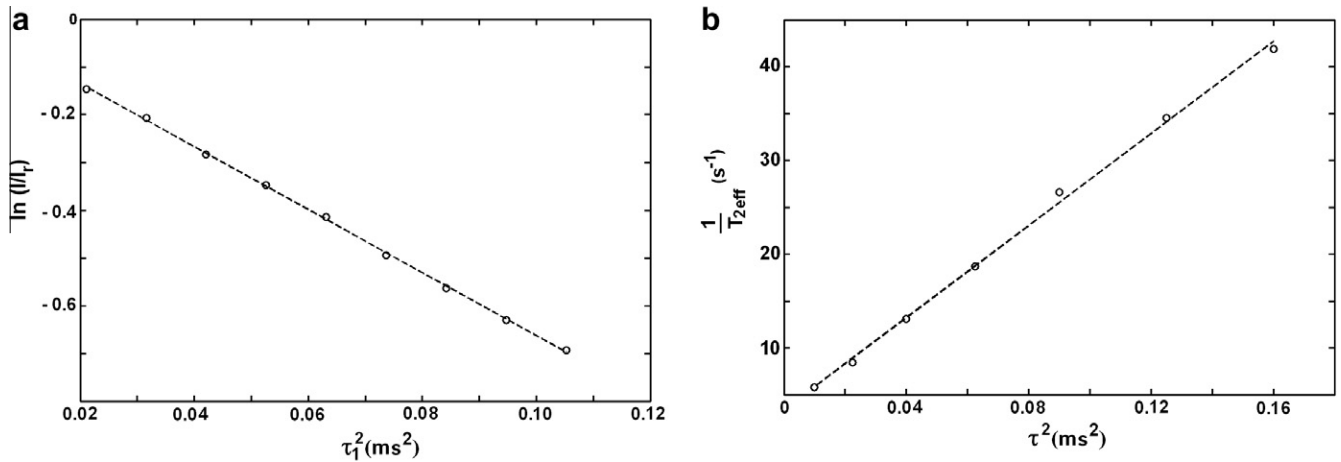


**Fig. 5.** Diffusion measurement using a distilled water phantom at 24.5 mm over the magnet, assuming a diffusion coefficient of  $2.07 \times 10^{-9} \text{ m}^2/\text{s}$ . The measured value of the gradient,  $G = 219 \text{ G/cm}$ , for SGSTE-CPMG sequence (a) and  $G = 223 \text{ G/cm}$  for CPMG with variable  $\tau$  (b) agree with the magnetic field measurement ( $G = 218 \text{ G/cm}$ ).

5 mm from the magnet center to the left, right, front and back has also been plotted (Fig. 4b). Fig. 4c shows the magnetic field plotted along horizontal lines ( $x$  and  $z$  directions) at three different heights over the magnet (1.3, 2.3 and 3.3 cm). The variation of the magnetic field is around 0.4% in the  $x$  direction and 1% along  $z$ . When the measurement point is moved to the right the error reached 1.7% for the plane closer to the magnet, which may be caused by small differences between the external blocks.

In order to obtain the desired constant gradient, the central block was displaced 2 mm down from the surface. The magnet blocks were spaced employing a fiberglass spacer to avoid acoustic ringing as described in [27,28]. The outer case is still aluminum but because the case walls are further away from the RF coil they do not produce any appreciable ringing.

Diffusion measurements employing a 4 ml sample of distilled water were carried out at heights of 15.5, 20, 24.5 and 29 mm over the magnet. The surface coil and the sample were displaced in tandem with retuning as necessary for each position. The sample was placed over the coil with its long dimension in the  $x$  axis. Gradient values of 217, 220, 219 and 222 G/cm respectively were measured, from SGSE-CPMG measurements using a known water diffusion coefficient of  $2.07 \times 10^{-9} \text{ m}^2/\text{s}$  at 21 °C.

In addition, a diffusion measurement employing CPMG for different  $\tau$  values was undertaken for a 24.5 mm sample height. The measured gradient in this simple case was 223 G/cm. Fig. 5 shows

the results of the measurement at this position for SGSE-CPMG (Fig. 5a) and CPMG with variable  $\tau$  (Fig. 5b). A good agreement is observed between the measurement from the three axis magnetic field plotter and the calculated gradient derived from both diffusion measurements. Small variations in the gradient value can be associated with noise or small changes in temperature during the experiment.

Fig. 6 presents a time-dependent diffusion coefficient measurement for two different types of rock core plugs and a reference sample of water. According to these results, fitting to Eq. (5), the volume to surface ratio in these rocks was determined to be around  $9.7 \mu\text{m}$  for Bentheimer and  $7 \mu\text{m}$  for Berea which result, assuming spherical pores, from radii of  $30 \mu\text{m}$  and  $20 \mu\text{m}$  respectively. These results agree with previous reports about these types of rocks in homogenous fields [29].

A simple unilateral CPMG measurement was also undertaken to determine the porosity in both samples. For the Bentheimer rock the porosity was 28% while for Berea it was 27%. Table 1 summarizes the results of these measurements, including an estimation of  $T_1$  for each rock core plug.

Measurement of the time-dependent diffusion coefficient was carried out employing a solenoid probe oriented in the  $x$  axis, with similar results (Fig. 6b) to those obtained with the surface coil. This type of RF probe gave us the opportunity to explore different planes inside the core plug. These planes are much deeper than

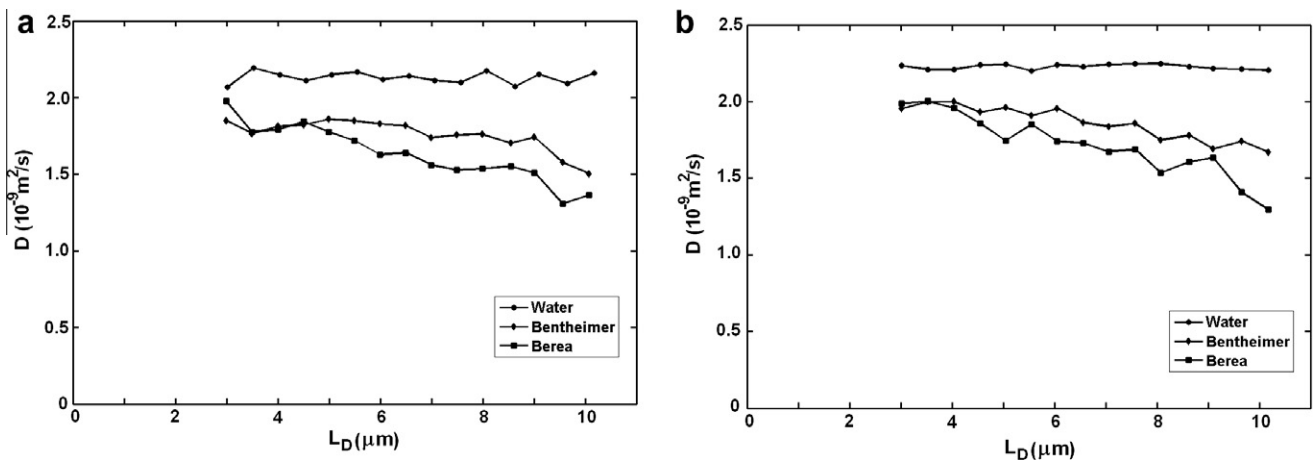


**Fig. 6.** Time-dependent diffusion coefficient for two different types of rocks and a reference sample of water. Apparent diffusion coefficients for 16 different diffusion times  $\tau_2$  were measured. The measurement plane for the surface coil (a) was 6 mm deep and 1.25 cm for the solenoid (b).



**Table 1**  
Comparison between Berea and Bentheimer core plug samples.

Sample	$T_1$ (ms)	Porosity (%)	V/S ratio ( $\mu\text{m}$ )	Pore radius ( $\mu\text{m}$ )
Bentheimer	600	28	9.7	30
Berea	120	27	7	20

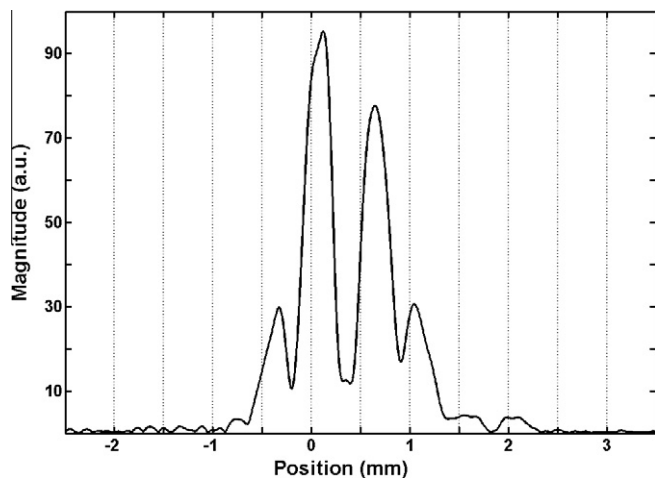


**Fig. 7.** Profile obtained from a simple test phantom of glass and rubber layers. The separation between peaks is 431  $\mu\text{m}$  except between the central peaks (625  $\mu\text{m}$ ) because of the presence of two layers of glass at that position.

those accessible to the surface coil probe. The plane position can be easily chosen by displacing the sample with respect to the magnet or by changing the RF frequency. In this last case RF probe retuning is necessary. For the measurements in Fig. 6 the measurement plane was 6 mm deep for the surface coil and 1.25 cm deep for the solenoid. The SNR was similar in both measurements. This result shows that the solenoid might be considered as a good choice for some specific applications in UMR. A solenoid probe can be easily built to fit specific samples or set of samples and is a natural choice for cylindrical samples.

Fig. 7 shows a profile acquired with a small surface coil from a test phantom composed of layers of glass and silicone rubber as another example of the behavior and potential application of the extended constant gradient produced with the three magnet array. The separation between peaks is 431  $\mu\text{m}$  (40 kHz). The separation in the test phantom is 485  $\mu\text{m}$  (45 kHz). A wider space between the

central peaks (625  $\mu\text{m}$ ) can be observed because of the presence of two layers of glass at that position. The amplitude of the peaks is modulated by the frequency response of the probe.

One experimental goal is the use of UMR to interrogate central portions of rock core samples which may vary from 1 to 4 in. diameters. Given the rock core application, we seek a static field strength which is approximately 470 G ( $f_0 = 2$  MHz) which is standard for rock core measurements. Fig. 8 shows a plot of the magnetic field measured around the center of a magnet designed for UMR constant gradient experiments at 2 MHz. In this case the gradient is 63 G/cm and the constant gradient region is 4 cm in extent, with a maximum deviation of 1 G from linear behavior. The lateral variation of the magnetic field in this case is 0.4% in a 1 cm diameter around the center. The reduction in the gradient value was achieved by doubling the width of the magnet blocks.

It is worthwhile to note that for lower gradient values, where the separation between the external blocks should be increased, a reduction in the overall magnetic field intensity should be expected. In this case, increasing the thickness of the blocks, which means a bigger and heavier array, will increase their effective separation and produce a degree of compensation for the loss in field intensity. On the other hand, small arrays can produce higher strength gradients at higher fields but over a shorter distance. Therefore, all these factors should be taken into account to produce the best array according to the application.

#### 4. Conclusions

A new and very simple way of creating constant magnetic field gradients in unilateral magnets has been introduced. Constant gradients of more than 3 cm extent can be achieved in a very simple and safe way. Diffusion measurements for different positions over the magnet employing SGSTE-CPMG, and CPMG with variable  $\tau$ , have been employed to characterize the gradient employing magnetic resonance. Good agreement has been obtained with both sequences and with the magnetic field measured with a magnetic field sensor. Practical applications for core plug characterization employing a surface coil and a solenoid have been presented. The results show that the solenoid is a good candidate to explore deep inside the samples employing unilateral magnetic resonance.

#### 5. Experimental

N48 NdFeB magnets (Yuxiang Magnetic Materials Ind. Co. Ltd., Xiamen, China) of  $10 \times 5 \times 3$  cm size were chosen for the external

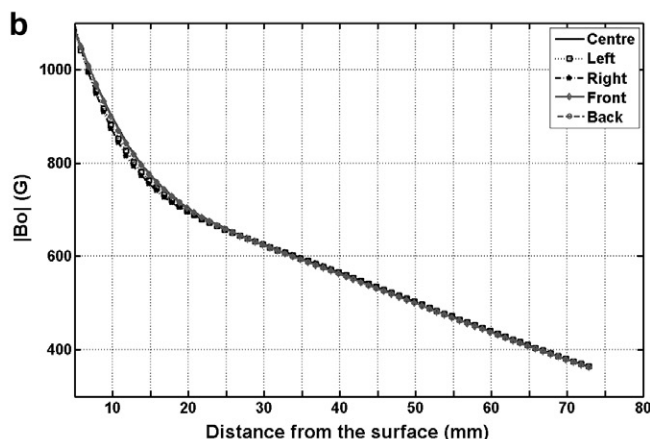
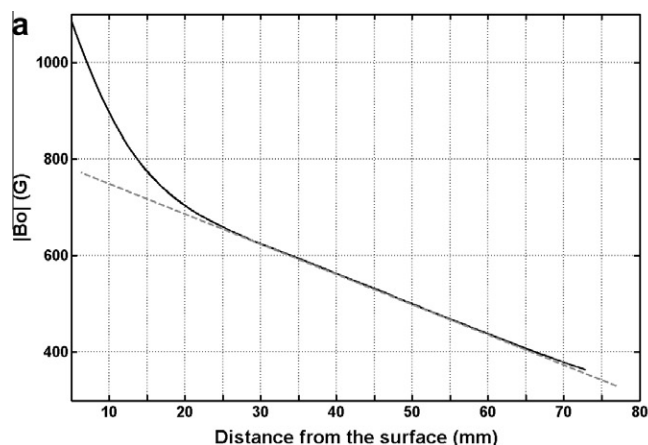


**Fig. 8.** Constant gradient produced by a three magnet array designed for a 2 MHz resonance frequency. The constant gradient of 63 G/cm and 4 cm extent are plotted in (a). The gradient for vertical lines spaced 5 mm from the center are plotted in (b).

blocks. A  $10 \times 5 \times 2$  cm block was employed for the central magnet. The array was placed in an aluminum box with magnet blocks separated by 4.76 mm thick fiberglass spacers.

The magnetic field distribution along a 4.5 cm vertical line over the center of the magnet was measured employing a three axis magnetic field probe (Lake Shore Cryotronics Inc., Westerville, USA) on a three axis plotter (Velmex Inc., Bloomfield, USA). Four additional measurements were carried out on vertical lines spaced 5 mm from the center of the magnet to evaluate the behavior of the gradient outside the central line. Additionally, the magnetic field measured along horizontal lines in the  $x$  and  $z$  direction at 1.3, 2.3 and 3.3 cm above the magnet was also measured. The spatial resolution for each measurement was 1 mm.

In order to evaluate the gradient strength by NMR, a diffusion measurement in a distilled water sample, at heights of 15.5, 20, 24.5 and 29 mm over the magnet, was undertaken employing both SGSTE-CPMG and CPMG with variable  $\tau$ . The sample container was 4 cm long with base of 1 cm on each side. It was placed in the center of the magnet with its long dimension in the  $x$  direction. The gradient value was calculated, assuming a water diffusion coefficient of  $2.07 \times 10^{-9} \text{ m}^2/\text{s}$  at 21 °C.

An extra diffusion measurement employing only CPMG with variable  $\tau$  with the above distilled water sample at 24.5 mm from the surface was completed for comparison. Seven data points were acquired for measuring the value of the gradient. For each data point a CPMG measurement with a different  $\tau$  was carried out to determine the effective  $T_2$  ( $T_{2\text{eff}}$ ). The  $\tau$  value was varied from 0.1 to 0.4 ms with an increase of 50  $\mu\text{s}$  between points. The time of measurement was 40 min, which can be reduced by decreasing the number of  $\tau$  values employed, the number of scans, and the repetition time.

A measurement of time-dependent diffusion coefficient was carried out employing core plugs of two different water saturated rocks (Bentheimer and Berea) and a sample of distilled water as a reference. The three samples employed for this measurement were 2.52 cm in diameter and 7.5 cm in length.

The static gradient stimulated echo sequence combined with CPMG (Fig. 3) and a 16 step phase table as suggested by Hurlimann [21] was employed. A reference signal at a short  $\tau_2$  ( $\tau_{2r} = 0.5$  ms) was acquired. The  $\tau$  value for the CPMG part of the sequence ( $\tau_1$ ) was set to 80  $\mu\text{s}$  for all measurements.

The number of scans was maintained at 64, with 400 echoes in the CPMG acquisition. For each diffusion measurement 9 different  $\tau_1$  values were employed. With these parameters and a repetition time of 10 s the measurement time was around 3 h. This duration may be reduced by decreasing the number of  $\tau_1$  values employed, the number of scans, and the repetition time. Additionally, employing a probe with shorter dead time would allow adding more echoes in the CPMG part of the sequence increasing the SNR and reducing the time of measurement.

For the time-dependent diffusion coefficient measurement 16 acquisitions for different  $\tau_2$  values, including the reference, were carried out. Both  $\tau_1$  and  $\tau_2$  values were chosen to obtain an equally spaced distribution of data points in all the measurements.

In order to determine the porosity of both samples a distilled water reference, same size as the core plugs, was employed. The CPMG decay for both core plugs and the reference were extrapolated to time zero. The ratio of amplitude for the core plugs and the reference expressed in percent was assumed as a measurement of porosity. Core plug measurements with 350 echoes, 128 averages and echo time of 0.2 ms, required 2 min for Berea and 6 min for Bentheimer core plug. A solenoid was employed as a probe.

A profile employing a small surface coil, 7 mm in diameter, was obtained from a phantom of simple layers of silicone rubber and glass. The thickness of the rubber and glass layers were 320 and 165  $\mu\text{m}$  respectively. For the acquisition, a CPMG sequence with

echo time of 0.2 ms and 300 echoes was employed. All the echoes were added to increase the SNR. A Fourier transform was applied to the resultant echo in order to obtain the profile. The measurement time was approximately 10 s.

The data acquisition was performed on a Minispec console (Bruker Analytik GmbH, Rheinstetten, Germany) with an external preamplifier (MITEQ, Hauppauge, USA). A surface coil of 2 cm diameter was employed for both radiofrequency transmission and reception. For measurements of the core plugs a solenoid probe of 3 cm in diameter, 3 cm long, was also employed. The pulse length was maintained at the same value for the RF pulses, with the maximum output power (250 W) for the 180°, in all the measurements. For the surface coil the pulse length was 5  $\mu\text{s}$  and 4.2  $\mu\text{s}$  for the solenoid. For the small surface coil employed for profiling, the pulse length was 2  $\mu\text{s}$ .

## Acknowledgments

JCG and BJB thank the Atlantic Innovation Foundation and ACOA for supporting this work. Saudi Aramco and Green Imaging Technologies are also thanked for sponsorship. BJB thanks NSERC for a Discovery grant and the Canada Chairs program for a research chair in MRI of materials.

## References

- [1] R.L. Kleinberg, A. Sezginer, D.D. Griffin, M. Fukuhara, Novel NMR apparatus for investigating an external sample, *J. Magn. Reson.* 97 (1992) 466–485.
- [2] R. Haken, B. Blumich, Anisotropy in tendon investigated in vivo by a portable NMR scanner, the NMR-MOUSE, *J. Magn. Reson.* 144 (2) (2000) 195–199.
- [3] P.F. de J. Cano-Barrita, A.E. Marble, B.J. Balcom, J.C. García, I.V. Mastikhin, M.D.A. Thomas, T.W. Bremner, Embedded NMR sensors to monitor evaporable water loss caused by hydration and drying in Portland cement mortar, *Cem. Concr. Res.* 39 (2009) 324–328.
- [4] S. Rahmatallah, Y. Li, H.C. Seton, I.S. Gregory, R.M. Aspdén, Measurement of relaxation times in foodstuffs using a one-sided portable magnetic resonance probe, *Eur. Food Res. Technol.* 222 (2006) 298–301.
- [5] G. Eidmann, R. Savelsberg, P. Blumler, B. Blumich, The NMR MOUSE, a mobile universal surface explorer, *J. Magn. Reson.* A 122 (1996) 104–109.
- [6] W.H. Chang, J.H. Chen, L.P. Hwang, Single-sided mobile NMR with a Halbach magnet, *Magn. Reson. Imaging* 24 (2006) 1095–1102.
- [7] E. Fukushima, J.A. Jackson, Unilateral Magnet Having a Remote Uniform Field Region for Nuclear Magnetic Resonance, US Patent 6489,872, 2002.
- [8] J.A. Jackson, L.J. Burnett, J.F. Harmon, Remote (inside-out) NMR. III. Detection of nuclear magnetic resonance in a remotely produced region of homogeneous magnetic, *J. Magn. Reson.* 41 (1980) 411–421.
- [9] A.E. Marble, I.V. Mastikhin, B.G. Colpitts, B.J. Balcom, An analytical methodology for magnetic field control in unilateral NMR, *J. Magn. Reson.* 174 (2005) 78–87.
- [10] A.E. Marble, I.V. Mastikhin, B.G. Colpitts, B.J. Balcom, A compact permanent magnet array with a remote homogeneous field, *J. Magn. Reson.* 186 (2007) 100–104.
- [11] J. Perlo, F. Casanova, B. Blumich, Ex situ NMR in highly homogeneous fields:  $^1\text{H}$  spectroscopy, *Science* 315 (2007) 1110–1112.
- [12] P.J. Prado, One-dimensional Imaging with palm-size probe, *J. Magn. Reson.* 144 (2000) 200–206.
- [13] B. Blumich, V. Anferov, S. Anferova, M. Klein, R. Fehete, M. Adams, F. Casanova, Simple NMR-mouse with a bar magnet, *Concr. Magn. Reson. B* 15 (2002) 255–261.
- [14] F. Casanova, B. Blumich, Two-dimensional imaging with a single-sided NMR probe, *J. Magn. Res.* 163 (2003) 38–45.
- [15] J. Perlo, F. Casanova, B. Blumich, 3D imaging with a single-side sensor: an open tomograph, *J. Magn. Reson.* 166 (2004) 228–235.
- [16] J. Perlo, F. Casanova, B. Blumich, Profiles with microscopic resolution by single-sided NMR, *J. Magn. Reson.* 176 (2005) 64–70.
- [17] P.J. McDonald, B. Newling, Stray field magnetic resonance imaging, *Rep. Prog. Phys.* 61 (1998) 1441–1493.
- [18] A.E. Marble, I.V. Mastikhin, B.G. Colpitts, B.J. Balcom, A constant gradient unilateral magnet for near-surface MRI profiling, *J. Magn. Reson.* 183 (2006) 228–234.
- [19] J.C. García-Naranjo, B.J. Balcom, I.V. Mastikhin, B.G. Colpitts, Three-magnet Array for Unilateral Magnetic Resonance, 9th Colloquium of Mobile NMR, August 30–September 4, Montana, USA, 2009.
- [20] R. Kimmich, E. Fischer, One- and two-dimensional pulse sequences for diffusion experiments in the fringe field of superconducting magnets, *J. Magn. Reson. Ser. A* 106 (1994) 229–235.

- [21] M.D. Hurlimann, L. Venkataramanan, Quantitative measurement of two-dimensional distribution functions of diffusion and relaxation in grossly inhomogeneous fields, *J. Magn. Reson.* 157 (2002) 31–42.
- [22] Lukasz J. Zielinski, M.D. Hurlimann, Short-time restricted diffusion in a static gradient and the attenuation of individual coherence pathways, *J. Magn. Reson.* 171 (2004) 107–117.
- [23] R. Kimmich, W. Unrath, G. Schnur, E. Rommel, NMR measurement of small self-diffusion coefficients in the fringe field of superconducting magnets, *J. Magn. Reson.* 91 (1991) 136–140.
- [24] M.D. Hurlimann, D.D. Griffin, Spin Dynamics of Carr-Purcell-Meibon-Gill-like sequences in grossly inhomogeneous  $B_0$  and  $B_1$  fields and application to NMR well logging, *J. Magn. Reson.* 143 (2000) 120–135.
- [25] D.G. Rata, F. Casanova, J. Perlo, D.E. Demco, B. Blumich, Self-diffusion measurement by a mobile single-side NMR sensor with improved magnetic field gradient, *J. Magn. Reson.* 180 (2006) 229–235.
- [26] G. Laicher, D.C. Ailion, A.G. Cutillo, Water Self-diffusion measurement in excised rat lungs, *J. Magn. Reson. Ser. B* 111 (1996) 243–253.
- [27] M.L. Buess, G.L. Petersen, Acoustic ringing effect in pulsed nuclear magnetic resonance probes, *Rev. Sci. Instrum.* 49 (1978) 1151–1155.
- [28] E. Fukushima, S.B.W. Roeder, Spurious ringing in pulse NMR, *J. Magn. Reson.* 33 (1979) 199–203.
- [29] H. Liaw, R. Kulkarni, S. Chen, T. Watson, Characterization of fluid distributions in porous media by NMR techniques, *AIChE J.* 42 (1996) 538–546.